Published in final edited form as:

Top Magn Reson Imaging. 2016 February ; 25(1): 31–37. doi:10.1097/RMR.0000000000000076.

Hyperpolarization MRI:

Preclinical Models and Potential Applications in Neuroradiology

Vesselin Z. Miloushev, MD, PhD, **Kayvan R. Keshari, PhD**, and **Andrei I. Holodny, MD**

Memorial Sloan Kettering Cancer Center, New York, NY.

Abstract

Hyperpolarization is a novel technology that can dramatically increase signal to noise in magnetic resonance. The method is being applied to small injectable endogenous molecules, which can be used to monitor transient in vivo metabolic events, in real time. The emergence of hyperpolarized ^{13}C-labeled probes, specifically ^{13}C pyruvate, has enabled monitoring of core cellular metabolic events. Neuro-oncological applications have been demonstrated in preclinical models. Many more applications of this technology are envisioned, with transformative potential in magnetic resonance imaging.

Keywords

^{13}C pyruvate; brain tumor metabolism; hyperpolarization MRI; preclinical models

Magnetic resonance signals are relatively weak compared with other spectroscopic or imaging technologies such as acoustic, optical, emission, or transmission methods. Historically, magnetic resonance has required high magnetic fields, high concentrations of spins, or lengthy acquisition times to allow for signal averaging, and sufficient signal to noise. Magnetic resonance imaging (MRI) is typically performed for water protons because of the relatively higher gyromagnetic ratio of protons among other nuclei and the high concentration of water in the human body. Proton MRI spectroscopy can detect a number of molecules that occur at high concentrations, usually in the 1 to 10 mM range. However, many interesting molecules are undetectable simply due to the inherent requirement of high concentrations. Because of the relatively low thermal equilibrium spin polarization (approximately 0.0003% for protons per Tesla, at body temperature), considerable gains in signal can be made by increasing the spin polarization to nearly unit values, even if the benefit is transient. Hyperpolarization increases signal in magnetic resonance by increasing spin polarization. Hyperpolarization technology is currently being applied to endogenous molecules, which can be isotopically enriched and hyperpolarized to dramatically increase their signal to noise allowing real-time monitoring of their metabolism. The promise of hyperpolarization technology is to harness the unique ability of nuclear magnetic resonance spectroscopy to distinguish chemical moieties on the basis of chemical shift and to characterize their dynamic properties in vivo.

Reprints: Vesselin Z. Miloushev, MD, PhD, Memorial Sloan Kettering Cancer Center, New York, NY (miloushv@mskcc.org).

The authors report no conflicts of interest.

HYPERPOLARIZATION TECHNOLOGY

Methods of Nuclear Spin Polarization

Several methods exist for increasing nuclear spin polarization. The current methods are applied to small molecules that are polarized ex vivo, and subsequently administered, similar to contrast agents, although with emergent properties as metabolic biomarkers. Although the effect is transient, this method allows observation of metabolism in vivo.

The dynamic nuclear polarization (DNP) method is one of the most widespread due to its versatility, as it can be applied to a wide variety of molecules. DNP operates on the principle of the Nuclear Overhauser Effect.[1] In his seminal work, Overhauser postulated the transfer of spin polarization from electron spins to nuclear spins by microwave irradiation of the electron spins. The current dissolution DNP method performs this spin polarization transfer at low temperatures, where the electron spins have very high polarization levels. During the polarization transfer, the target molecule and an electron donor molecule are maintained as an amorphous solid that is then rapidly dissolved just before use.[2] This method regularly achieves polarization on the order of 20% to 40 % (eg, compared with approximately 0.00008% polarization for ^{13}C per Tesla at body temperature), but this efficiency can vary between different molecules.

In parahydrogen-induced polarization (PHIP), spin polarization is transferred from parahydrogen to the target molecule via a chemical reaction.[3–6] The process can be accomplished rapidly, yielding high levels of polarization, but due to the requirements of the chemical reaction, only a limited set of molecules can be polarized using this technique.

Lastly, hyperpolarization of noble gases such as helium and xenon can be accomplished by spin-exchange via optical pumping.[7,8] Before the development of the DNP method, hyperpolarized helium gas was the only hyperpolarized technology applied to human imaging. However, the feasibility of monitoring metabolism with hyperpolarized ^{13}C using the DNP method has recently been demonstrated in humans by several groups.

LIMITS AND TECHNICAL CONSIDERATIONS

A hyperpolarizable molecule is described by the position of the NMR-active nucleus. The most abundant isotope of hydrogen, namely proton, is a spin-1/2 nucleus and is natively NMR observable. However, the spin-1/2 NMR-active isotope of carbon, namely ^{13}C, is only approximately 1.1% naturally abundant, necessitating isotopic enrichment of the target molecule to further increase signal to noise. Thus, the position of isotopic enrichment is important in characterizing the hyperpolarized molecule. For example, [1-^{13}C] pyruvate means that the first carbon position in pyruvate is enriched for ^{13}C. This atom's nuclear spin would be the target of the hyperpolarization process. The molecule is usually abbreviated HP pyruvate, but the distinction as to which carbon atom is isotopically enriched is important. This determines the expected spectral profile and fate of the hyperpolarized label in downstream metabolic products, as the hyperpolarized atom is transferred between metabolites. Endogenous molecules are preferred for in vivo studies of metabolism, because they can usually be administered at near or supra-physiological concentrations without

deleterious effects. Moreover, endogenous molecules provide information on native metabolic processes in the organism.

The effective lifetime of the molecule is dictated by its T_1 time constant, as this determines how much spin polarization is lost from the time of initial hyperpolarization to actual imaging. Feasibility currently requires selection of molecules with T_1 time constants at least on the order of seconds, with longer lifetimes being obviously preferred. As a requisite, the hyperpolarized molecule is prepared just before use, to minimize relaxation losses. Furthermore, the relaxation properties of different dynamic states of the molecule will dictate to what extent they are detectable. However, promising work in transforming magnetization into long-lived states may circumvent the T_1 limits of certain molecules.[9–11]

Imaging of hyperpolarized metabolites has unique challenges. The magnetic resonance spectroscopic imaging (MRSI) sequence must rapidly accomplish both spatial and spectral localization. Because the hyperpolarized magnetization relaxes with the T_1 constant and cannot be recovered, improved signal to noise is usually obtained from shorter experiments. Some of the recent improvements in the field include fly-back echoplanar spectroscopic imaging, double spin echo technique, spectral-spatial excitation, and compressed sensing.[12–15] Dedicated coils are often required in hyperpolarization experiments, as imaging is usually carried out on nonproton nuclei, such as ^{13}C or ^{15}N.

The utility of any molecule for hyperpolarized imaging depends on its polarization and relaxation properties, its imaging properties, as well as its safety, biological availability, and ultimately the metabolic information that it provides (Table 1).

RECENT DEVELOPMENTS: ^{13}C PROBES

The development of injectable hyperpolarized carbon probes marked a paradigm shift in hyperpolarization MRI, departing from prior applications of hyperpolarized agents augmenting anatomic imaging by increasing signal to noise. Hyperpolarized carbon probes have the ability to detect both precursors and downstream products of central metabolic reactions in vivo and are beginning to establish the field of hyperpolarized metabolic imaging.[16] Initial attempts were complicated by uncertain delivery of probes through the blood-brain barrier, and thus utility was limited to angiographic applications.[17,18] However, the emergence of ^{13}C pyruvate, an endogenous molecule that crosses the blood-brain barrier and is actively metabolized, allowed monitoring of central cellular energy metabolism.[19] Pyruvate has emerged as a canonical hyperpolarized metabolic probe with distinct advantages demonstrated for neurological applications in preclinical animal models.

PYRUVATE

Pyruvate is a naturally occurring small molecule with a central role in metabolism. Endogenous pyruvate is present in 35±25 μM concentrations in normal human serum and has been implicated in neuroprotection from oxidative stress, excitatory toxicity, and inflammation.[20,21] Pyruvate enters cells through the specialized monocarboxylase family of transporters, which are differentially expressed in neurons and astrocytes.[22]

Pyruvate, which can be produced after initial steps of glucose metabolism, is located at the metabolic “cross-roads” of aerobic and anaerobic metabolism. It can enter the tricarboxylic acid cycle (TCA, aerobic metabolism) by decarboxylation and formation of acetyl CoA. This reaction also produces carbon dioxide, which is rapidly converted to and detected as bicarbonate, catalyzed by carbonic anhydrase. Alternatively, pyruvate can be converted to lactate (anaerobic metabolism) by lactate dehydrogenase.

Isotopically enriching pyruvate at the first carbon position, [1-^{13}C]-pyruvate, allows detection of metabolism to [1-^{13}C]-lactate (anaerobic metabolism) via lactate dehydrogenase, [1-^{13}C]-alanine via alanine synthase, and ^{13}C-bicarbonate, indicating entry into TCA cycle (aerobic metabolism and oxidative phosphorylation, Fig. 1). Alternatively, isotopically enriching pyruvate at the second position, [2-^{13}C]-pyruvate allows detection of additional TCA cycle intermediates Fig. 1.[23]

In the anesthetized rodent brain, hyperpolarized pyruvate is preferentially metabolized to lactate, with maximum production occurring approximately 20 to 40 seconds following injection, Fig. 2. However, bicarbonate (indicative of aerobic metabolism), and to a lesser extent alanine, can be detected at low levels.[24,25] Flux of pyruvate into the TCA cycle can be increased pharmacologically, and it is possible that similar modulations occur under different metabolic demands.[26]

Using hyperpolarized pyruvate, preclinical models have shown that relative to perfusion, the metabolism of pyruvate to lactate is greater in the brain than the extracranial soft tissues, underscoring the highly metabolic nature of the brain. Extending the work of rodent models, metabolism of pyruvate in the anesthetized nonhuman primate brain has demonstrated conversion of pyruvate to lactate,[27] Fig. 3. It remains to be determined, however, whether preferential metabolism of pyruvate to lactate occurs in the normal human brain, how this is modulated by metabolic coupling of neurons and astrocytes, and how this is coupled to neuronal activation and neural networks.

PRECLINICAL MODELS IN NEURO-ONCOLOGY

Preclinical studies of hyperpolarized metabolic probes in neurooncology have demonstrated applications to both diagnosis and treatment response in rodent brain tumor models. One of the first demonstrations of in vivo metabolism using hyperpolarized pyruvate MRI in a preclinical rodent xenograft tumor model showed different metabolism in tumor tissue and normal tissues.[28] This led to the hypothesis that the different tissues have different metabolic profiles, which can be used to differentiate microscopic differences in vivo. The culmination of this work was the first demonstration of hyper-polarized pyruvate metabolism in human prostate cancer, where pyruvate to lactate metabolism occurs at an increased rate in tumor cells (^{13}C pyruvate is currently under an investigational new drug application).[29] Importantly, as a general paradigm, preclinical models have demonstrated that metabolic alterations can precede genetic transformations.[30] The potential of HP metabolic imaging is thus not only to detect abnormal cancer metabolism but also to identify premalignant states.

Hyperpolarized Pyruvate in Brain Tumors

Cancer metabolism is in general different from the metabolism of normal cells, and these differences appear to be essential for tumorigenesis.[31,32] Cancer cells upregulate glucose metabolism and inactivate pyruvate dehydrogenase (PDH), blocking entry of pyruvate into the TCA cycle, and preferentially metabolizing pyruvate to lactate.[33] Several brain tumors have been shown to follow this general feature of abnormal metabolism and preferentially perform anaerobic glycolysis and reductive glutaminolysis.[34,35] However, among brain tumors, lactate production and metabolic profiles can vary substantially.[36,37] There is further evidence of metabolic differences in glioma stem cells, and metabolic heterogeneity within individual brain tumors.[15,38]

Preclinical applications of HP [1-^{13}C]-pyruvate to lactate metabolism have been demonstrated in rodent xenograft glioma models,[15,39,40] Fig. 4. Production of lactate correlates with the MIB-1 index, and there are differences between xenograft glioma cell lines (decreased lactate production was seen in the more invasive U251MG model than the U87MG model). Moreover, the kinetics of hyperpolarized [1-^{13}C]-pyruvate metabolism are significantly higher in xenograft glioma models than normal brain parenchyma.[41]

Importantly, HP [1-^{13}C]-pyruvate metabolism has been used to assess treatment response in human glioma orthotopic xenograft models.[40] In animals treated with temozolamide, the glioblastoma xenograft tumors rapidly demonstrated decreased pyruvate-to-lactate ratios, before reduction in tumor size. Further, HP [1-^{13}C]-pyruvate metabolism has been reproduced in the assessment of response of more invasive glioma orthotopic xenograft models.[42] In that study, treatment with everolimus, an mTOR inhibitor that modulates glycolysis, demonstrated significantly decreased pyruvate-to-lactate ratios. These models provide rationale for use of HP metabolic probes in treatment response.

Hyperpolarized Probes for Molecular Diagnosis

Hyperpolarized agents have the ability to image specific tumor metabolism because complex enzymatic post-translational and genetic modifications are necessary for cancer cells to proliferate. This has recently come to the forefront of neuro-oncology because gain-of-function isocitrate dehydrogenase (IDH) mutations occur in low-grade gliomas and some secondary glioblastomas.[43] The mutation results in accumulation of the oncometabolite 2-hydroxyglutarate (2HG) by conversion from the TCA intermediate alpha-ketoglutarate (aKG). Because the 2HG metabolite occurs at high levels in mutant cells, it can be detected by nonhyperpolarized ^{1}H MRSI.[44,45] However, sensitivity is determined by high concentrations of this molecule and detection reflects a stationary pool. Alternatively, HP methods have the potential to detect 2HG and other oncometabolites with higher sensitivity, and importantly to detect instantaneous metabolism rather than a static pool. The IDH-1 mutation has been detected by both directly using HP [1-^{13}C] alpha-ketoglutarate and indirectly monitoring [1-^{13}C] glutamate in IDH1 mutant human glioma cell lines and orthotopic xenografts,[46,47] though much work will be needed to clinically translate these methods.

Hyperpolarized Probes Beyond Pyruvate

Beyond HP pyruvate, many additional molecules central to metabolism can be hyperpolarized with varied applications.[16,48,49] These include TCA intermediates, such as ^{13}C αketoglutarate, ^{13}C succinate, and ^{13}C fumarate.[18,46,50] Furthermore, within gliomas, variation in concentration of several amino acids, including glycine and serine, suggests their potential use with respect to determining tumor grade.[37]

Glutamine, an amino acid that is central to metabolism however, may have the most generalizable application in brain tumors. Glutamine is the most abundant amino acid in human plasma, and glutamine metabolism is essential to several brain tumors, including glioma, neuroblastoma, and lymphoma.[35] Hyperpolarized glutamine could be an alternative to recently demonstrated ^{18}F-glutamine for gliomas.[51,52]

Beyond specific metabolism, hyperpolarized probes can inform on global properties of brain umors such as pH balance or cellular oxidative potential. The brain is known to have complex activity dependent shifts in pH and acid–base balance, which is often abnormal in tumors and their vicinity.[53] Several hyperpolarized probes of pH are being actively developed. Arguably, one of the simplest is monitoring the balance of bicarbonate and CO_2, an equilibrium that is pH dependent.[54] Cellular reduction-oxidation potential has been evaluated by monitoring the reverse-conversion of vitamin C (reduced form) from dehydroascorbate (oxidized form).[55] Preclinical models have demonstrated that the anesthetized rodent brain has high reductive potential compared with other organs, Fig. 5.[56] Clearly, these hyperpolarized probes may have important neurological applications beyond neuro-oncology.

POTENTIAL APPLICATIONS

Hyperpolarized metabolic imaging can be obtained concurrently with high resolution anatomic ^{1}H MRI, and has the potential to revolutionize virtually every current neuroradiological application. Localization of altered metabolism has the potential to detect and characterize not only macroscopic but also microscopic abnormalities. This is particularly important when localized treatment is planned, and margins are critically important. Beyond neuro-onco-logical applications, HP metabolic imaging could provide increased specificity in localization related epilepsy. HP pyruvate maybe useful given evidence of differential monocarboxylase transporter expression in epileptogenic regions.[57,58] HP metabolic imaging could replace the current use of ^{18}FDG which is hampered by high background activity in the brain, in many applications.

Clearly, appropriately designed hyperpolarized probes may detect enzymatic alterations in cases of inborn errors of metabolism with high specificity. This type of imaging would go further than genotypic confirmation by characterizing the penetrance/phenotypic severity of any mutation and monitoring the effect of treatment. Furthermore, HP metabolic imaging has an inherent ability for multiplexing, because several hyperpolarized probes can be administered at the same time, provided that they have spectral resolution.[59] As endogenous HP probes are nontoxic, and the signal from HP probes rapidly decays or can be easily “deactivated,” repeat administrations can be performed.

HP metabolic imaging would be particularly useful in any situation wherein anatomic imaging findings are nonspecific or often lag behind clinical metabolic improvement. In infection and neuroinflammation, metabolic imaging could provide rapid evidence of treatment response. Metabolic imaging could detect stress in compensatory reserves of homeostasis before irreversible damage. This is particularly important in imaging of normal aging, neuro-degenerative diseases, traumatic brain injury, various encephalopathies, and ischemia/stroke. For example, decreased aerobic glycolysis is implicated in neurodegenerative diseases and pyruvate metabolism has been shown to be age dependent in preclinical models.[60,61] Furthermore, many neurodegenerative diseases have alterations in the cellular oxidation state and development of free radicals. HP probes monitoring redox potential, such as ^{13}C DHA/vitamin C, may have important applications.[55] Finally, hyperpolarized vascular imaging using perfusional agents such as ^{13}C urea could offer a nontoxic, high signal-to-noise, and easily quantifiable alternative to paramagnetic contrast or spin-labeling techniques.[17]

Functional HP metabolic imaging of the normal human brain may offer distinct advantages to current fMRI, which uses T_2* imaging of the BOLD effect. Primary benefits are increased signal to noise and high temporal sensitivity. Metabolic activation in response to stimulus has been demonstrated in the rat brain using hyperpolarized xenon.[62] However, the information from metabolic HP probes, such as pyruvate, would be conceivably different, because specific metabolism related to neuronal activation would be imaged. Synaptic plasticity, for example, is known to depend on aerobic glycolysis,[60] and the metabolism of neurons and astrocytes is known to be highly coupled.[63–66] Hyperpolarized functional imaging may be more quantitative and may better characterize the complex activations of the human brain.

CONCLUSIONS

Hyperpolarization MRI is a newly emerging technology with potentially transformative benefits for patients. This technology relies on dramatic amplification of the MRI signal from small molecules, allowing their use as probes of specific albeit transient metabolic events. Emerging neuro-oncological applications to brain tumors have been demonstrated in preclinical models. Many more applications are envisioned that can harness the unique power of this technology.

ACKNOWLEDGMENT

MSK CancerCenter SupportGrant/Core Grant (P30CA008748).

REFERENCES

1. Overhauser AW. Polarization of nuclei in metals. Phys Rev. 1953; 92:411–415.
2. Ardenkjaer-Larsen JH, Fridlund B, Gram A, et al. Increase in signal-to-noise ratio of >10,000 times in liquid-state NMR. Proc Natl Acad Sci U S A. 2003; 100:10158–10163. [PubMed: 12930897]
3. Bowers CR, Weitekamp DP. Transformation of symmetrization order to nuclear-spin magnetization by chemical reacion and nuclear-magnetic-resonance. Phys Rev Lett. 1986; 57:2645–2648. [PubMed: 10033824]

4. Bowers CR, Weitekamp DP. Parahydrogen and synthesis allow dramatically enhanced nuclear alignment. J Am Chem Soc. 1987; 109:5541–5542.
5. Chekmenev EY, Hovener J, Norton VA, et al. PASADENA hyperpolarization of succinic acid for MRI and NMR spectroscopy. J Am Chem Soc. 2008; 130:4212–4213. [PubMed: 18335934]
6. Adams RW, Aguilar JA, Atkinson KD, et al. Reversible interactions with para-hydrogen enhance NMR sensitivity by polarization transfer. Science. 2009; 323:1708–1711. [PubMed: 19325111]
7. Happer W, Miron E, Schaefer S, et al. Polarization of the nuclear spins of noble-gas atoms by spin exchange with optically pumped alkali-metal atoms. Phys Rev A. 1984; 29:3092–3110.
8. Walker TG, Happer W. Spin-exchange optical pumping of noble-gas nuclei. Rev Modern Phys. 1997; 69:629–642.
9. Carravetta M, Levitt MH. Theory of long-lived nuclear spin states in solution nuclear magnetic resonance. I. Singlet states in low magnetic field. J Chem Phys. 2005; 122:214505. [PubMed: 15974752]
10. Feng Y, Davis RM, Warren WS. Accessing long-lived nuclear singlet states between chemically equivalent spins without breaking symmetry. Nat Phys. 2012; 8:831–837. [PubMed: 23505397]
11. Stevanato G, Hill-Cousins JT, Hakansson P, et al. A nuclear singlet lifetime of more than one hour in room-temperature solution. Angew Chem Int Ed Engl. 2015; 54:3740–3743. [PubMed: 25631745]
12. Cunningham CH, Chen AP, Albers MJ, et al. Double spin-echo sequence for rapid spectroscopic imaging of hyperpolarized 13C. J Magn Reson. 2007; 187:357–362. [PubMed: 17562376]
13. Larson PE, Kerr AB, Chen AP, et al. Multiband excitation pulses for hyperpolarized 13C dynamic chemical-shift imaging. J Magn Reson. 2008; 194:121–127. [PubMed: 18619875]
14. Yen YF, Kohler SJ, Chen AP, et al. Imaging considerations for in vivo 13C metabolic mapping using hyperpolarized 13C-pyruvate. Magn Reson Med. 2009; 62:1–10. [PubMed: 19319902]
15. Park I, Hu S, Bok R, et al. Evaluation of heterogeneous metabolic profile in an orthotopic human glioblastoma xenograft model using compressed sensing hyperpolarized 3D 13C magnetic resonance spectroscopic imaging. Magn Reson Med. 2013; 70:33–39. [PubMed: 22851374]
16. Keshari KR, Wilson DM. Chemistry and biochemistry of 13C hyperpolarized magnetic resonance using dynamic nuclear polarization. Chem Soc Rev. 2014; 43:1627–1659. [PubMed: 24363044]
17. Mansson S, Johansson E, Magnusson P, et al. 13C imaging-a new diagnostic platform. Eur Radiol. 2006; 16:57–67. [PubMed: 16402256]
18. Bhattacharya P, Chekmenev EY, Perman WH, et al. Towards hyperpolarized (13)C-succinate imaging of brain cancer. J Magn Reson. 2007; 186:150–155. [PubMed: 17303454]
19. Zhang, H. Hyperpolarized Sodium 1-[13C]Pyruvate. National Center for Biotechnology Information (US); Bethesda, MD: 2004. p. 2004-2013.
20. Psychogios N, Hau DD, Peng J, et al. The human serum metabolome. PLoS One. 2011; 6:e16957. [PubMed: 21359215]
21. Zilberter Y, Gubkina O, Ivanov AI. A unique array of neuroprotective effects of pyruvate in neuropathology. Front Neurosci. 2015; 9:17. [PubMed: 25741230]
22. Hertz L, Dienel GA. Lactate transport and transporters: general principles and functional roles in brain cells. J Neurosci Res. 2005; 79:11–18. [PubMed: 15586354]
23. Park JM, Josan S, Grafendorfer T, et al. Measuring mitochondrial metabolism in rat brain in vivo using MR spectroscopy of hyperpolarized [2-(1)(3)C]pyruvate. NMR Biomed. 2013; 26:1197–1203. [PubMed: 23553852]
24. Hurd RE, Yen YF, Mayer D, et al. Metabolic imaging in the anesthetized rat brain using hyperpolarized [1-13C] pyruvate and [1-13C] ethyl pyruvate. Magn Reson Med. 2010; 63:1137–1143. [PubMed: 20432284]
25. Mayer D, Yen YF, Takahashi A, et al. Dynamic and high-resolution metabolic imaging of hyperpolarized [1-13C]-pyruvate in the rat brain using a high-performance gradient insert. Magn Reson Med. 2011; 65:1228–1233. [PubMed: 21500253]
26. Park JM, Recht LD, Josan S, et al. Metabolic response of glioma to dichloroacetate measured in vivo by hyperpolarized (13)C magnetic resonance spectroscopic imaging. Neuro Oncol. 2013; 15:433–441. [PubMed: 23328814]

27. Park I, Larson PE, Tropp JL, et al. Dynamic hyperpolarized carbon-13 MR metabolic imaging of nonhuman primate brain. Magn Reson Med. 2014; 71:19–25. [PubMed: 24346964]
28. Golman K, Zandt RI, Lerche M, et al. Metabolic imaging by hyperpolarized 13C magnetic resonance imaging for in vivo tumor diagnosis. Cancer Res. 2006; 66:10855–10860. [PubMed: 17108122]
29. Nelson SJ, Kurhanewicz J, Vigneron DB, et al. Metabolic imaging of patients with prostate cancer using hyperpolarized [1-13C]pyruvate. Sci Transl Med. 2013; 5:198ra108.
30. Hu S, Balakrishnan A, Bok RA, et al. 13C-pyruvate imaging reveals alterations in glycolysis that precede c-MYC induced tumor formation and regression. Cell Metab. 2011; 14:131–142. [PubMed: 21723511]
31. Warburg O. On the origin of cancer cells. Science. 1956; 123:309–314. [PubMed: 13298683]
32. Pelicano H, Martin DS, Xu RH, et al. Glycolysis inhibition for anticancer treatment. Oncogene. 2006; 25:4633–4646. [PubMed: 16892078]
33. Dang CV, Kim J-w, Gao P, et al. The interplay between MYC and HIF in cancer. Nat Rev Cancer. 2008; 8:51–56. [PubMed: 18046334]
34. Oudard S, Boitier E, Miccoli L, et al. Gliomas are driven by glycolysis: putative roles of hexokinase, oxidative phosphorylation and mitochondrial ultrastructure. Anticancer Res. 1997; 17(3C):1903–1911. [PubMed: 9216643]
35. DeBerardinis RJ, Mancuso A, Daikhin E, et al. Beyond aerobic glycolysis: transformed cells can engage in glutamine metabolism that exceeds the requirement for protein and nucleotide synthesis. Proc Natl Acad Sci. 2007; 104:19345–19350. [PubMed: 18032601]
36. Subhash MN, Rao BS, Shankar SK. Changes in lactate dehydrogenase isoenzyme pattern in patients with tumors of the central nervous system. Neurochem Int. 1993; 22:121–124. [PubMed: 8439765]
37. Chinnaiyan P, Kensicki E, Bloom G, et al. The metabolomic signature of malignant glioma reflects accelerated anabolic metabolism. Cancer Res. 2012; 72:5878–5888. [PubMed: 23026133]
38. Vlashi E, Lagadec C, Vergnes L, et al. Metabolic state of glioma stem cells and nontumorigenic cells. Proc Natl Acad Sci U S A. 2011; 108:16062–16067. [PubMed: 21900605]
39. Park I, Larson PE, Zierhut ML, et al. Hyperpolarized 13C magnetic resonance metabolic imaging: application to brain tumors. Neuro Oncol. 2010; 12:133–144. [PubMed: 20150380]
40. Park I, Bok R, Ozawa T, et al. Detection of early response to temozolomide treatment in brain tumors using hyperpolarized 13C MR metabolic imaging. J Magn Reson Imaging. 2011; 33:1284–1290. [PubMed: 21590996]
41. Park JM, Josan S, Jang T, et al. Metabolite kinetics in C6 rat glioma model using magnetic resonance spectroscopic imaging of hyperpolarized [1-13C]pyruvate. Magn Reson Med. 2012; 68:1886–1893. [PubMed: 22334279]
42. Chaumeil MM, Ozawa T, Park I, et al. Hyperpolarized 13C MR spectroscopic imaging can be used to monitor Everolimus treatment in vivo in an orthotopic rodent model of glioblastoma. Neuroimage. 2012; 59:193–201. [PubMed: 21807103]
43. Dang L, White DW, Gross S, et al. Cancer-associated IDH1 mutations produce 2-hydroxyglutarate. Nature. 2009; 462:739. [PubMed: 19935646]
44. Choi C, Ganji SK, DeBerardinis RJ, et al. 2-hydroxyglutarate detection by magnetic resonance spectroscopy in IDH-mutated glioma patients. Nat Med. 2012; 18:624–629. [PubMed: 22281806]
45. Andronesi OC, Kim GS, Gerstner E, et al. Detection of 2-hydroxyglutarate in IDH-mutated glioma patients by in vivo spectral-editing and 2D correlation magnetic resonance spectroscopy. Sci Transl Med. 2012; 4:116ra114.
46. Chaumeil MM, Larson PEZ, Yoshihara HAI, et al. Non-invasive in vivo assessment of IDH1 mutational status in glioma. Nat Commun. 2013; 4:2429–12429. [PubMed: 24019001]
47. Chaumeil MM, Larson PE, Woods SM, et al. Hyperpolarized [1-13C] glutamate: a metabolic imaging biomarker of IDH1 mutational status in glioma. Cancer Res. 2014; 74:4247–4257. [PubMed: 24876103]
48. Kurhanewicz J, Vigneron DB, Brindle K, et al. Analysis of cancer metabolism by imaging hyperpolarized nuclei: prospects for translation to clinical research. Neoplasia (New York NY). 2011; 13:81–97.

49. Salamanca-Cardona L, Keshari KR. (13)C-labeled biochemical probes for the study of cancer metabolism with dynamic nuclear polarization-enhanced magnetic resonance imaging. Cancer Metab. 2015; 3:9. [PubMed: 26380082]
50. Gallagher FA, Kettunen MI, Hu DE, et al. Production of hyperpolarized [1,4-13C2]malate from [1,4-13C2]fumarate is a marker of cell necrosis and treatment response in tumors. Proc Natl Acad Sci U S A. 2009; 106:19801–19806. [PubMed: 19903889]
51. Cabella C, Karlsson M, Canape C, et al. In vivo and in vitro liver cancer metabolism observed with hyperpolarized [5-(13)C]glutamine. J Magn Reson. 2013; 232:45–52. [PubMed: 23689113]
52. Venneti S, Dunphy MP, Zhang H, et al. Glutamine-based PET imaging facilitates enhanced metabolic evaluation of gliomas in vivo. Sci Transl Med. 2015; 7:274ra217.
53. Chesler M. Regulation and modulation of pH in the brain. Physiol Rev. 2003; 83:1183–1221. [PubMed: 14506304]
54. Gallagher FA, Kettunen MI, Day SE, et al. Magnetic resonance imaging of pH in vivo using hyperpolarized 13C-labelled bicarbonate. Nature. 2008; 453:940–943. [PubMed: 18509335]
55. Keshari KR, Sai V, Wang ZJ, et al. Hyperpolarized [1-(13)C]dehydroascorbate MR spectroscopy in a murine model of prostate cancer: comparison with (18)F-FDG PET. J Nucl Med. 2013; 54:922–928. [PubMed: 23575993]
56. Keshari KR, Kurhanewicz J, Bok R, et al. Hyperpolarized 13C dehydroascorbate as an endogenous redox sensor for in vivo metabolic imaging. Proc Natl Acad Sci U S A. 2011; 108:18606–18611. [PubMed: 22042839]
57. Lauritzen F, de Lanerolle NC, Lee TS, et al. Monocarboxylate transporter 1 is deficient on microvessels in the human epileptogenic hippocampus. Neurobiol Dis. 2011; 41:577–584. [PubMed: 21081165]
58. Lauritzen F, Heuser K, de Lanerolle NC, et al. Redistribution of monocarboxylate transporter 2 on the surface of astrocytes in the human epileptogenic hippocampus. Glia. 2012; 60:1172–1181. [PubMed: 22535546]
59. Wilson DM, Keshari KR, Larson PE, et al. Multi-compound polarization by DNP allows simultaneous assessment of multiple enzymatic activities in vivo. J Magn Reson. 2010; 205:141–147. [PubMed: 20478721]
60. Harris RA, Tindale L, Cumming RC. Age-dependent metabolic dysregulation in cancer and Alzheimer's disease. Biogerontology. 2014; 15:559–577. [PubMed: 25305052]
61. Jiang T, Cadenas E. Astrocytic metabolic and inflammatory changes as a function of age. Aging Cell. 2014; 13:1059–1067. [PubMed: 25233945]
62. Mazzanti ML, Walvick RP, Zhou X, et al. Distribution of hyperpolarized xenon in the brain following sensory stimulation: preliminary MRI findings. PLoS One. 2011; 6:e21607. [PubMed: 21789173]
63. Pellerin L, Bouzier-Sore AK, Aubert A, et al. Activity-dependent regulation of energy metabolism by astrocytes: an update. Glia. 2007; 55:1251–1262. [PubMed: 17659524]
64. Paulson OB, Hasselbalch SG, Rostrup E, et al. Cerebral blood flow response to functional activation. J Cereb Blood Flow Metab. 2010; 30:2–14. [PubMed: 19738630]
65. Belanger M, Allaman I, Magistretti PJ. Brain energy metabolism: focus on astrocyte-neuron metabolic cooperation. Cell Metab. 2011; 14:724–738. [PubMed: 22152301]
66. Turner DA, Adamson DC. Neuronal-astrocyte metabolic interactions: understanding the transition into abnormal astrocytoma metabolism. J Neuropathol Exp Neurol. 2011; 70:167–176. [PubMed: 21293295]
67. Park JM, Josan S, Jang T, et al. Volumetric spiral chemical shift imaging of hyperpolarized [2-c]pyruvate in a rat c6 glioma model. Magn Reson Med;. 2015 [Epub ahead of print].
68. Golman K, Ardenkjaer-Larsen JH, Petersson JS, et al. Molecular imaging with endogenous substances. Proc Natl Acad Sci U S A. 2003; 100:10435–10439. [PubMed: 12930896]

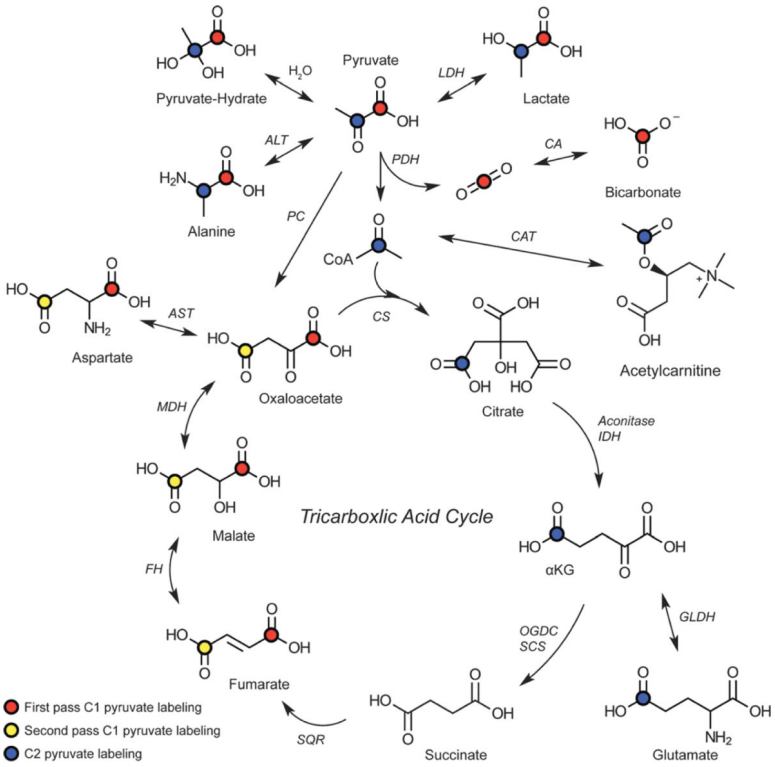

FIGURE 1.

Pyruvate metabolic fates diagram. Isotopically labeling pyruvate at the first carbon position permits detection of lactate (anaerobic metabolism) and bicarbonate (aerobic metabolism), as well as alanine some TCA intermediates. Isotopically labeling pyruvate at the second carbon position permits detection of additional TCA cycle intermediates. Reproduced with permission from *Chem Soc Rev* 2014; 43:1627–1659.

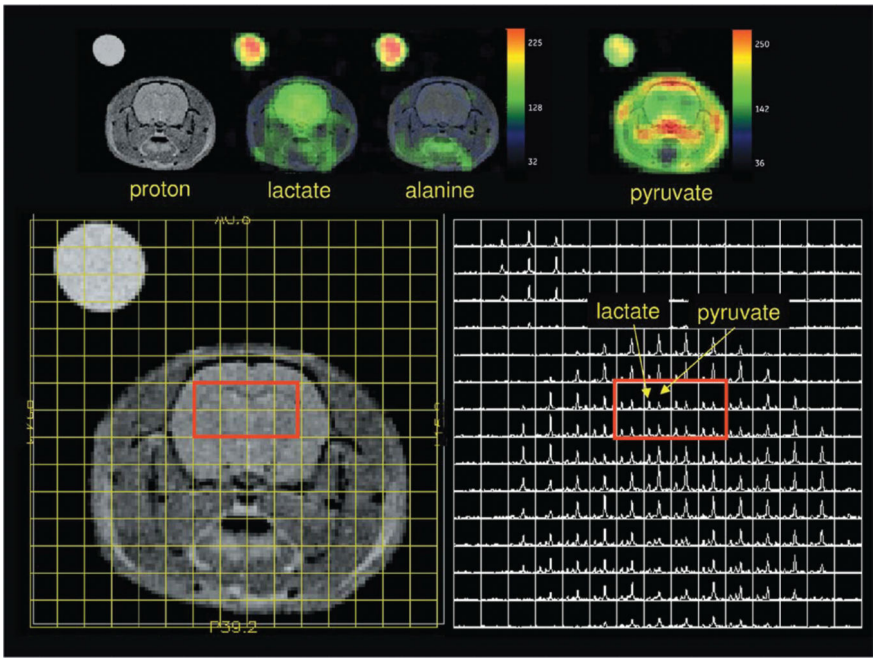

FIGURE 2.

Pyruvate metabolism in preclinical animal model. Hyperpolarized [1-^{13}C] pyruvate is preferentially metabolized to lactate in the anesthesized rat brain. Metabolic maps of lactate, alanine, and pyruvate are shown in the top row. The left lower panel shows ^{1}H anatomic imaging. The right lower panel shows the source magnetic resonance spectroscopic imaging (MRSI), with individual resonances corresponding to pyruvate and its metabolic product, lacatate. Reproduced with permission from *Magn Reson Med* 2010; 63:1137–1143.

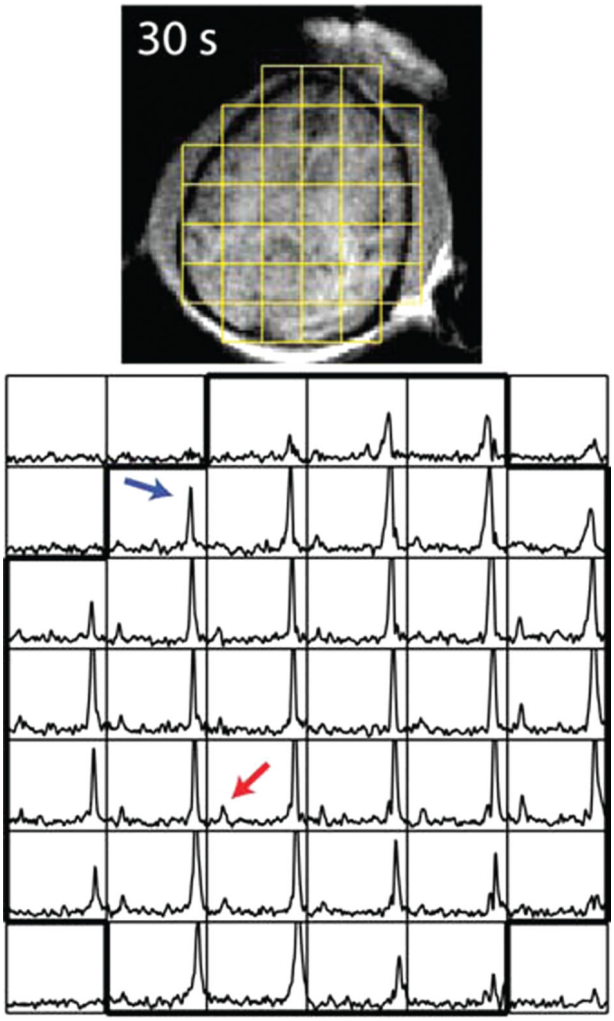

FIGURE 3.

Hyperpolarized pyruvate metabolism in the nonhuman primate brain. Pyruvate (black arrow) and its metabolic product lactate resonance (grey arrow) are detected. Top panel: ^{1}H anatomic image with overlayed MRSI grid. Bottom panel: corresponding MRSI. Reproduced with permission from *Magn Reson Med* 2014; 71:19–25.

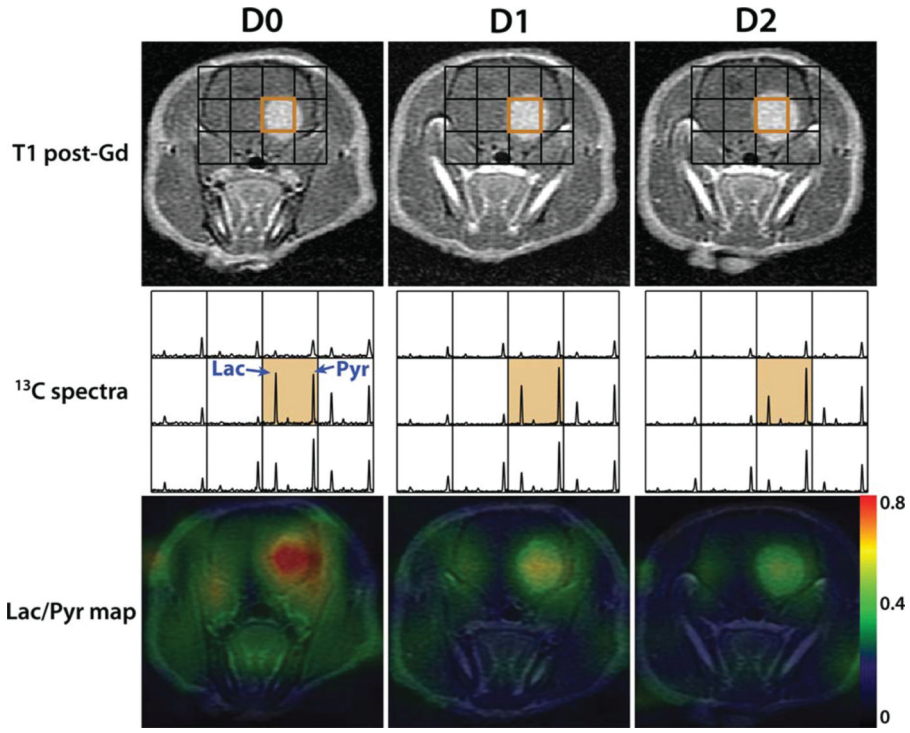

FIGURE 4.

Hyperpolarized pyruvate in assessment of treatment response. Hyperpolarized [1-^{13}C] pyruvate to lacate metabolism decreases following temozolamide treatment in a rat xenograft glioma model. The left, middle, and right columns show the changes at days 0, 1, 2 following 100 mg/kg temozolomide treatment. The top row shows contrast-enhanced images, with overlayed MRSI grid. The middle row shows corresponding spectra. The bottom row shows the corresponding metabolite maps. Reproduced with permission from *J Magn Reson Imaging* 2011; 33:1284–1290.

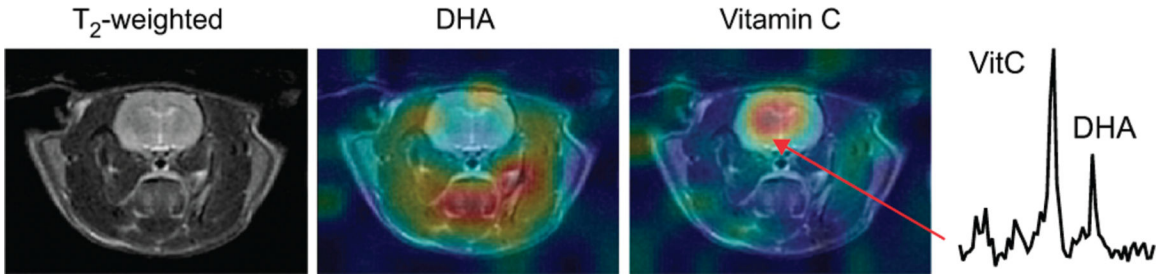

FIGURE 5.

Monitoring oxidative potential in the brain. The oxidized metabolic precursor dehydroascorbate (DHA) is rapidly reduced to Vitamin C in the anesthetized rat brain, indicating high reductive potential of the brain. Left image: ^{1}H anatomic imaging; middle image: DHA metabolite map; right image: Vitamin C metabolite map; left most panel: representative spectrum with Vitamin C and DHA resonances. Reproduced with permission from *Proc Natl Acad Sci U S A* 2011; 108: 18606–18611.

Table 1

Potential ^{13}C Hyperpolarized Applications in Neuroradiology

Potential Application	Probe	Downstream Metabolites	References
Glycolysis, Warburg effect	[1-^{13}C] pyruvate	Lactate, alanine, bicarbonate	15,24,39
Glycolysis, TCA cycle	[2-^{13}C] pyruvate	TCA intermediates	5,18,46,51,67
	[1-^{13}C] alpha-ketoglutarate		
	[1,4-^{13}C] fumarate		
Glutaminolysis	[1,5-^{13}C] glutamate/glutamine	Glutamate, TCA intermediates	47
Perfusion	^{13}C Urea	Intracellular/Extracellular pools	68
pH	^{13}C Bicarbonate	CO_2	54
Redox potential	[1-^{13}C] DHA	Vitamin C	56